

IN-PLANE CYCLIC TESTS OF CALCIUM SILICATE MASONRY WALLS

GUIDO MAGENES and PAOLO MORANDI

Department of Structural Mechanics, University of Pavia and EUCENTRE
Pavia, Italy

ANDREA PENNA

European Centre for Training and Research in Earthquake Engineering (EUCENTRE)
Pavia, Italy

SUMMARY

In-plane cyclic testing of large scale walls is the basic source of information on the lateral seismic behaviour of masonry buildings. A test setup for cyclic testing of masonry piers has been developed at the University of Pavia – EUCENTRE structural laboratories within the ESECMaSE Project framework. The new apparatus has been used in order to assess the lateral capacity of masonry piers of different slenderness, load and boundary conditions and with various typologies of blocks, mortar and constructive details. In this paper the results obtained from the tests of the first eight calcium silicate walls are presented. Different failure modes have been observed and the associated force-displacement capacity and energy dissipation properties are reported.

INTRODUCTION

The ESECMaSE Project is a research project funded by the European Commission within the Sixth Framework Programme, aiming at improving the knowledge on the lateral in-plane response of masonry walls and the global seismic behaviour of entire buildings. The project is mainly focused on three typologies of blocks produced in Europe for new constructions: hollow clay, calcium silicate and lightweight aggregate concrete blocks.

Within the ESECMaSE framework both numerical simulations and experimental tests are carried out by the project partners. The activity of the University of Pavia is mainly devoted to the in-plane cyclic testing of masonry piers. A total of 27 large scale walls will be tested.

In order to be able to control the walls boundary conditions (cantilever or double-fixed) and also to speed up the tests, a completely new test setup has been designed; a clear and repeatable procedure has been used for the whole testing campaign.

In this paper a description of both the test setup and the procedure is provided together with the results of the first group of eight unreinforced calcium silicate walls.

TEST SET-UP AND INSTRUMENTATION

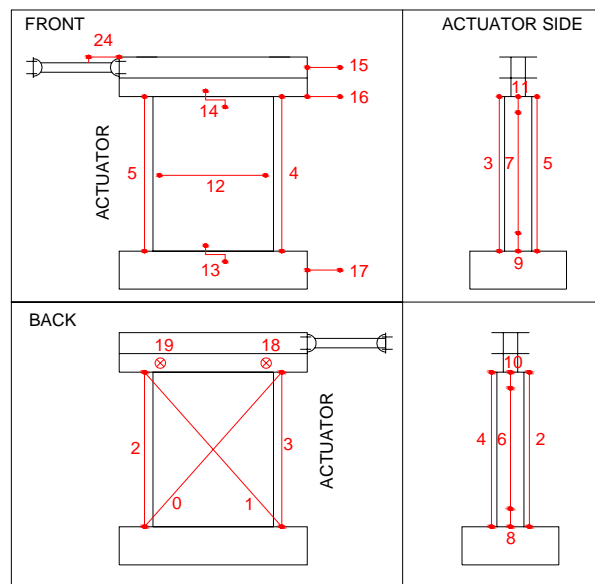
The in-plane cyclic tests were carried out in the EUCENTRE Laboratory for Seismic Testing of Large Structures. The installation of the new test setup took advantage of the three-dimensional configuration of the strong floor and the L-shaped strong walls.

The adopted test setup is shown in Figure 1(a). The walls are built on a 400 mm thick reinforced concrete footing which could be clamped to the strong floor by means of post-tensioned steel bars. A horizontally mounted servohydraulic actuator applies a horizontal shear force to the top of the wall through a composite steel spreader beam. The steel beam is stiffened with steel plates positioned orthogonally to the development of the beam. The wall is restrained from out-of-plane deflections by a sliding restrainer system. Two vertical servohydraulic actuators apply the vertical load on the wall, reacting on a steel frame fixed on one of the strong walls of the laboratory.

Figure 1(b) schematically shows the typical wall instrumentation. The horizontal load was measured by a load cell positioned in the horizontal actuator. Twenty five displacement transducers (linear potentiometers) were installed on each wall. The horizontal displacement at the top of the wall was measured by instruments 15, 16 and 24. Wall flexural deformations were monitored by instruments 2-11, whereas shear deformations were monitored by instruments 0 and 1. Relative sliding displacements between the wall and the footing, between the top beam and the wall and between the strong floor and the footing were monitored by instruments 13, 14 and 17 respectively. Control of out-of-plane displacements was monitored by instruments 18 and 19.



a)



b)

Figure 1. Test set-up and instrumentation

TESTING PROCEDURE

The testing procedure envisaged two different boundary conditions: a “double fixed” system (rotation restrained at the top beam) and a “cantilever” system (free rotation at the top) with a constant vertical load applied at the top with servohydraulic actuators. The horizontal load was applied using a servohydraulic actuator, with an initial force-controlled phase followed by a displacement-controlled loading history, performing three cycles for each target displacement level.

The top steel beam was connected to the wall by a layer of high strength gypsum mortar. The vertical force imposed by the vertical actuators was initially gradually applied in order to estimate the compressive Young’s modulus of masonry. In case of a cantilever system both

the forces of the right and left actuators are kept constant during the test and hence they are not dependent on the horizontal actuator force and displacement.

The double fixed system can be obtained by two alternative settings of the actuator control. The first one is based on a “static” criterion, obtained imposing the condition of zero bending moment at midheight of the wall. The second one, adopted for most of the tests, consists of a “kinematic” criterion, which involves a mixed force-displacement control, imposing both a constant vertical load and a condition of free translation with no rotation of the top beam.

The horizontal loading history is as follows. Before the test, an estimate of the maximum shear strength is made, and a first repetition of three fully reversed cycles is performed by imposing, in a force-controlled way, a horizontal force equal to one fourth of the maximum estimated strength. Horizontal displacements are recorded. The procedure is then switched to a displacement-controlled one, in which the target displacements are multiple of the displacement measured in the first force-controlled phase, repeating three cycles for each target displacement. This method aims to get sufficient points describing the ascending branch of the force-displacement envelope curve. Once the specimen approaches its maximum shear strength the further target displacements are then chosen from a predefined sequence of drift-based displacement levels.

The duration of each cycle is kept constant incrementing the actuator displacement rate proportionally to the cycle target displacement as also done in past experimental campaigns (Tomazevic *et al.*, 1993). The tests are stopped in case of critical damage conditions or at a horizontal top displacement larger than 2.0% drift.

TEST SPECIMENS AND MATERIAL PROPERTIES

A total of eight calcium-silicate masonry walls were tested. The dimensions and the details for the walls are summarized in Table 1. All specimens were 175 mm thick and 2.5 m high. The testing campaign included six walls (CS01-C606) with a length of 1.25 m and two walls (CS07 and CS08) with a length of 2.5m. Square 248x248 mm calcium-silicate units have been used (see Figure 2). All walls were made with thin layer mortar bedjoints (about 2 mm thick) with unfilled head joints. Only for wall CS05 head joints had been filled by thin layer mortar. Three levels of vertical mean compression stress σ_v were applied: 0.5, 1.0 and 2.0 MPa.

All walls were tested with double fixed boundary conditions except walls CS06 and CS08 which were tested as cantilever systems.

According to the compressive tests carried out at the University of Munich (Grabowski, 2005), the mean compression strength of the units was 26.5 MPa. Three diagonal compression tests on masonry square wallets (1.0 x 1.0 m) with unfilled head joints were carried out in Pavia. The conventional diagonal tensile strength of masonry was computed as $f_t = P/(2 \cdot t \cdot l)$ where P is the maximum diagonal compression load, t and l are the thickness and the length of the wallets respectively. The mean value of the diagonal tensile strength was 0.27 MPa.

Table 1. Calcium-silicate masonry piers.

Wall	l [m]	t [m]	h [m]	σ_v [MPa]	Unit size [mm]	Bed joints	Head joints	Bound. Conditions
CS 01	1.25	0.175	2.5	1.0	248x175x248	Thin layer	Unfilled	Double fixed
CS 02	1.25	0.175	2.5	1.0	248x175x248	Thin layer	Unfilled	Double fixed
CS 03	1.25	0.175	2.5	0.5	248x175x248	Thin layer	Unfilled	Double fixed
CS 04	1.25	0.175	2.5	2.0	248x175x248	Thin layer	Unfilled	Double fixed
CS 05	1.25	0.175	2.5	1.0	248x175x248	Thin layer	Filled (Thin)	Double fixed
CS 06	1.25	0.175	2.5	1.0	248x175x248	Thin layer	Unfilled	Cantilever
CS 07	2.50	0.175	2.5	1.0	248x175x248	Thin layer	Unfilled	Double fixed
CS 08	2.50	0.175	2.5	1.0	248x175x248	Thin layer	Unfilled	Cantilever



Figure 2. Type of calcium-silicate unit used for the walls ($l \times t \times h = 248 \times 175 \times 248$ mm)

EXPERIMENTAL RESULTS

Ductility, displacement capacity and energy dissipation issues are here discussed with reference to the specific experimental failure mechanisms. The results of the cyclic tests on the eight calcium-silicate masonry piers in terms of hysteretic force-displacement curves are presented in Figures 3 to 10 (the top displacement δ measured at the lowest edge of the steel beam is considered). The pictures of the piers at the end of the tests are also reported.

Failure modes of the piers

The double fixed condition on wall CS01 was applied using the “static” criterion described above, i.e. keeping the point of zero moment at mid-height of the pier. The wall failed with a sudden diagonal crack interesting both the joints and the units. Evaluating the data after the test, it appeared clear that keeping constant the point of contra-flexure at mid-height, a very large rotation of the top beam occurred due to inherent unavoidable non-symmetry of the wall, thus resulting in unrealistic kinematic boundary conditions at the top. In addition to that, with such system it was impossible to follow the post-peak branch of the curve, due to loss of control after the formation of the diagonal crack. As a consequence, starting from wall CS02, the tests were carried out with the “kinematic” criterion, i.e. keeping the top beam horizontal. The failure of wall CS02 was characterized by corner-to-corner diagonal shear cracks. The cracks developed in the units and in the mortar bedjoints. The units at the top right and top left corner of the wall rotated producing a concentrated compression load that caused diagonal cracks at the units below. Spalling of the units at the centre of the pier occurred and the development of many wide diagonal cracks in the units at the centre of the panel caused the brittle collapse of the wall, with a sudden drop of the shear force.

Wall CS03 was characterized by the opening of the unfilled head joints which became evident at the top displacement $\delta = \pm 10$ mm. The head- and bed-joint cracks formed a pattern of stepped diagonal cracks along the height of the wall. These cracks closed during unloading. Increasing the top displacement the cracks became rather wide and no further increase of shear was possible. When the top displacement exceeded 15 mm, cracks developed in the units at the centre of the panel, producing large strength degradation and collapse of the wall.

In wall CS04, a higher vertical load ($\sigma_v = 2$ MPa) was applied, and the wall failed with diagonal shear cracks in the masonry units from corner to corner of the wall, at very small top displacement (just beyond 4.0 mm). Spalling of some units at the centre of the wall also occurred. Large strength and stiffness degradation occurred after diagonal cracking. Before attaining this displacement level no evident damage was present, therefore it is possible to state that this wall behaved almost similar to an elastic-brittle system.

Wall CS05 remained undamaged, with the exception of some tension cracks in bedjoints, up to a horizontal top displacement of 35 mm. When this displacement level was exceeded, the wall failed suddenly in shear with the development of a diagonal crack formed in the mortar bedjoints and in the units. Before this damage, the force-displacement curve presented “S-shaped” cycles without any relevant energy dissipation, similar to a typical rocking behaviour.

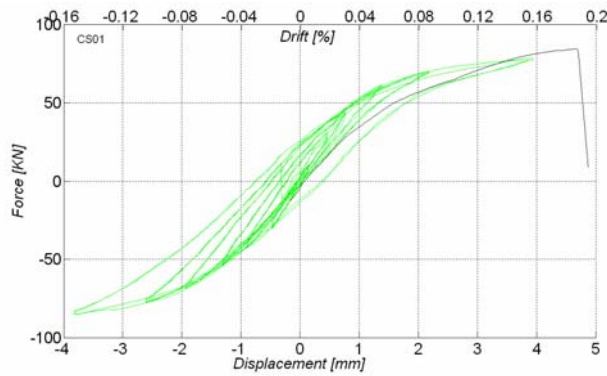


Figure 3 Wall CS01. Double fixed, $l=1.25$ m, $\sigma_v=1.0$ MPa

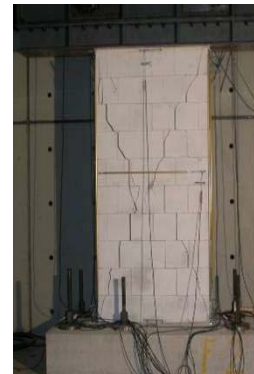
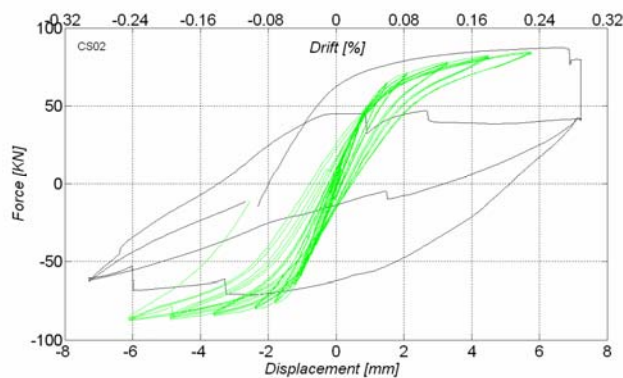


Figure 4 Wall CS02. Double fixed, $l=1.25$ m, $\sigma_v=1.0$ MPa

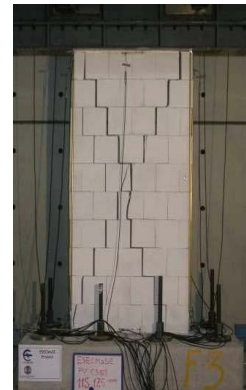
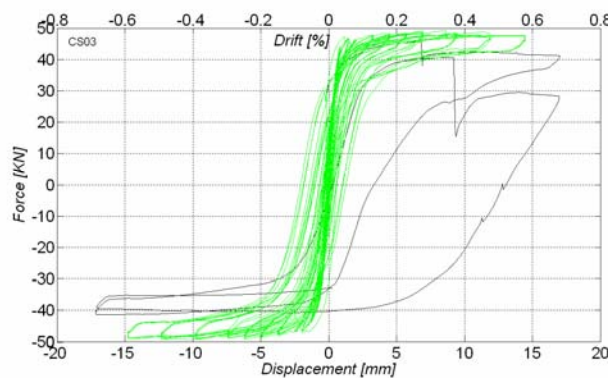


Figure 5 Wall CS03. Double fixed, $l=1.25$ m, $\sigma_v=0.5$ MPa

Although wall CS05 was constructed and tested with the same characteristics of wall CS01 and wall CS02, head joints filled by mortar allowed to attain a larger displacement capacity in comparison with the displacements found in the tests on wall CS01 and wall CS02.

Wall CS06 was tested as a cantilever system. No diagonal cracks occurred during the test and the wall displayed a typical rocking behaviour without any significant strength degradation or relevant energy dissipation. With a top displacement larger than 40 mm (corresponding to a drift of 1.6 %) a wide horizontal crack was clearly visible in the bottom right corner of the panel due to tension stresses. The test was interrupted when the top displacement attained about 50 mm (2% drift) for reasons due to the stroke limits of the transducers; at that stage the wall was substantially undamaged (except for the horizontal crack) and probably it would have been still possible to further increase the displacement demand.

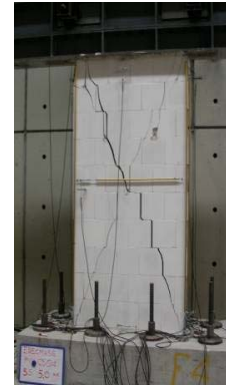
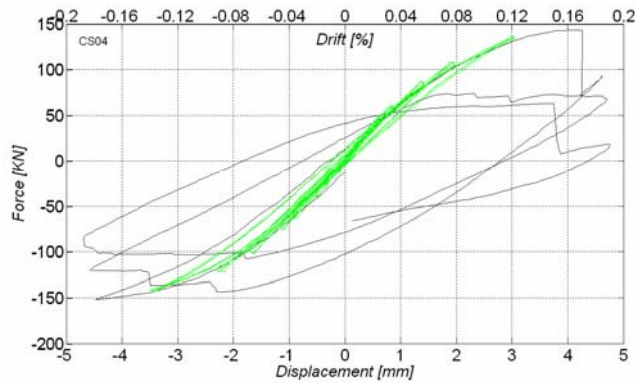


Figure 6 Wall CS04. Double fixed, $l=1.25$ m, $\sigma_v=2.0$ MPa

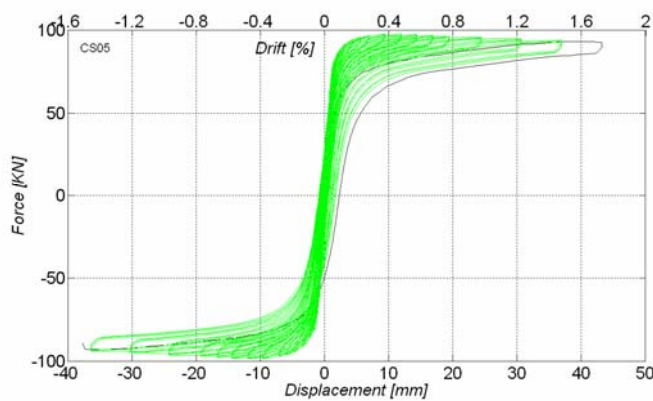


Figure 7 Wall CS05. Double fixed, $l=1.25$ m, $\sigma_v=1.0$ MPa, filled head joints

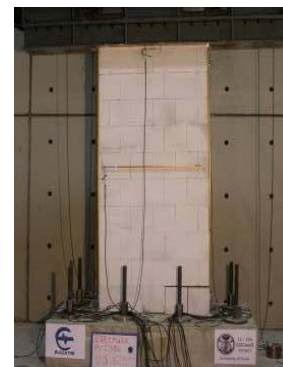
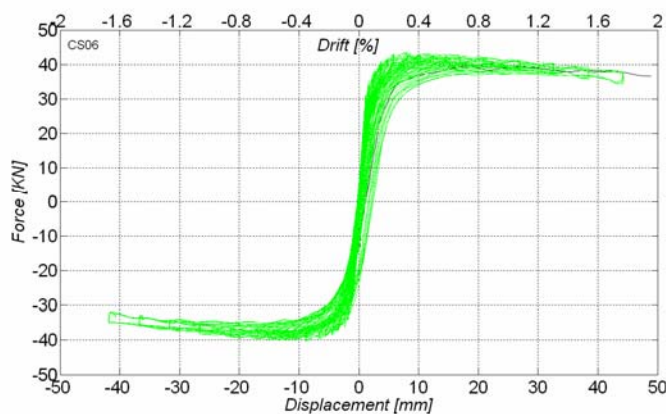


Figure 8 Wall CS06. Cantilever, $l=1.25$ m, $\sigma_v=1.0$ MPa

Wall CS07 was characterized by a force-displacement response typical of rocking failure. At a horizontal displacement of about ± 17 mm the opening of the unfilled head joints was very evident. Cracking of bedjoints concurred to form a system of stepped diagonal cracks along the wall. These cracks closed during unloading. The hysteresis cycles showed very low energy dissipation and no strength degradation since no cracks in the units or sliding in bedjoints occurred. The test was interrupted when the top displacement was 30 mm (1.2% drift) because very wide vertical cracks in the joints had developed and separation of a large wedge of masonry took place, with the danger of a partial collapse of the wedge itself.

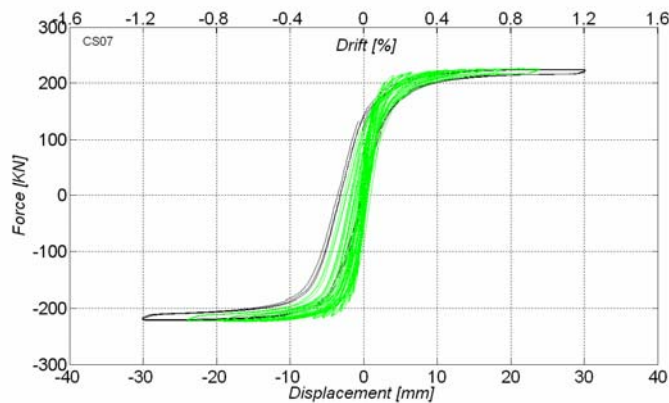


Figure 9 Wall CS07. Double fixed, $l=2.50$ m, $\sigma_v=1.0$ MPa

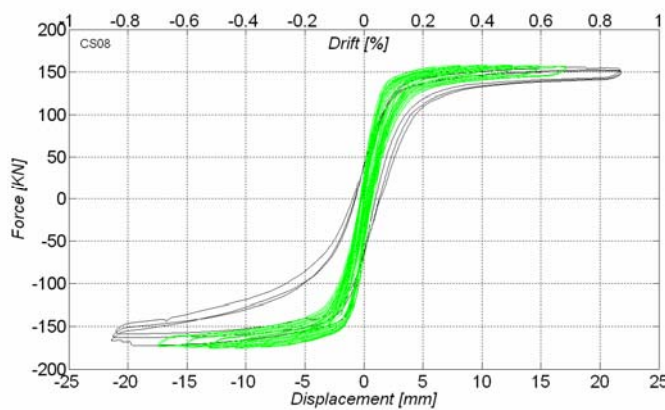


Figure 10 Wall CS08. Cantilever, $l=2.50$ m, $\sigma_v=1.0$ MPa

Wall CS08 had same geometric characteristic and same vertical load of wall CS07 but it was tested as a cantilever system. At a horizontal displacement of about ± 12 mm opening of the unfilled head joints became visible to form stepped inclined cracks along the height of the wall. Low energy dissipation and no strength degradation occurred. Cracks closed during unloading. Rocking-type response of the wall was displayed. Beyond a top displacement of 20 mm several diagonal cracks in the units of the right bottom half part of the wall developed and in these last cycles a slightly higher energy dissipation was displayed.

Ductility and deformation capacity

A common approach to interpret the in-plane response of masonry walls is to idealize the cyclic envelope of the hysteresis loop with a bilinear envelope. In Figure 11 a possible definition of the parameters of the bilinear curve is given, as per Magenes & Calvi, 1997. The elastic stiffness is obtained by drawing the secant to the experimental envelope at $0.75V_u$, where $V_u = 0.9 \cdot V_{max}$. The ultimate ductility is defined as $\mu_u = \delta_u / \delta_e$ where the ultimate displacement δ_u corresponds to a strength degradation equal to 20% of V_u . Ductility and displacement capacity were calculated for each wall considering the first, the second and third cycle envelope. Since the results in terms of displacement capacity are very similar for the three cycles, only the results of the third cycle are reported (see Table 2). The failure mechanism of walls CS07 and CS08 has been classified conventionally as “hybrid” due to the coexistence of a force-displacement response typical of rocking systems with the presence of stepped inclined cracks interesting bed- and headjoints.

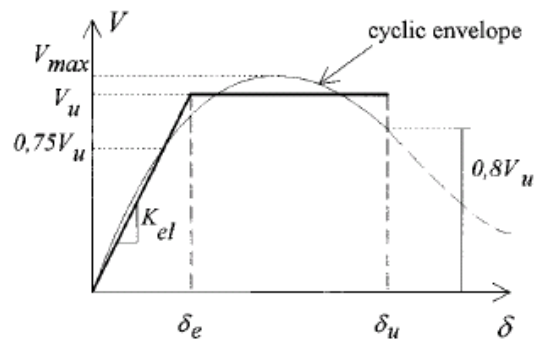


Figure 11. Hysteresis envelope and its bilinear idealization [Magenes and Calvi, 1997].

Table 2. Ultimate ductility and ultimate displacement calculated for the third cycle experimental envelope. The superscripts ⁺ and ⁻ refer to the positive and negative shear-displacement envelope. H is the height of the piers.

Test	k_{el}^+ [KN/mm]	k_{el}^- [KN/mm]	δ_e^+ [mm]	δ_e^- [mm]	δ_u^+ [mm]	δ_u^- [mm]	μ_u^+	μ_u^-	$\mu_{u,min}$	δ_u^+/H	δ_u^-/H	$(\delta_u/H)_{min}$	Fail. Mech.
CS01	51	39	1.4	2.0	3.9	3.8	2.8	1.9	1.9	0.0016	0.0015	0.0015	SHEAR
CS02	48	57	1.4	1.3	7.2	7.3	4.6	5.3	4.6	0.0029	0.0029	0.0029	SHEAR
CS03	75	63	0.6	0.7	14.5	14.7	24.2	21.0	21.0	0.0058	0.0059	0.0058	SHEAR
CS04	61	62	2.0	2.1	3.6	4.3	1.8	2.1	1.8	0.0014	0.0017	0.0014	SHEAR
CS05	77	74	1.1	1.2	36.8	35.9	32.4	30.2	30.2	0.0147	0.0144	0.0144	HYBRID
CS06	26	27	1.5	1.3	44.2	41.9	29.8	31.7	29.8	0.0177	0.0168	0.0168	FLEXURE
CS07	149	155	1.4	1.3	30.1	30.1	22.1	23.1	22.1	0.0120	0.0120	0.0120	HYBRID
CS08	58	84	2.4	1.9	21.6	21.0	8.9	11.3	8.9	0.0087	0.0084	0.0084	HYBRID

High ductility values were found for almost all walls including some of those failing in shear. The lower values were reported for wall CS01 and CS04 for which a sudden drop in the strength was due to brittle diagonal shear crack (CS01 was affected also by loss of control once the diagonal crack developed), whereas walls CS02 despite failing with diagonal cracking, displayed a slightly higher ductility and drift capacity. Wall CS03, characterized by progressive damage propagation for opening and closing of the vertical unfilled head joints attained a remarkable ductility and drift. Wall CS05 characterized by the presence of head joints filled by mortar was able to largely exceed 1% drift with a flexure-dominated response before the occurrence of a diagonal shear crack.

Very high values of ductility and drift capacity were found for walls CS06 and CS07 and CS08. This behaviour is typical of rocking-flexure failure. The maximum displacement attained for such walls was more related to the experimental set-up displacement capacity or to the local damage more than significant shear strength degradation. Wall CS08, tested as a cantilever, attained unexpectedly a lower drift and ductility than its double fixed counterpart (CS07), although the drift capacity is quite high compared to the walls failing in shear.

In the case of walls failing by shear, the drift capacities were very low, especially in the case of high values of axial load. Wall CS04 attained a value of drift less than 0.14%.

Similar elastic stiffness k_{el} (as defined in Figure 11) was found for walls having same dimensions and same boundary conditions independently from the axial load.

Energy dissipation capacity

The dissipated hysteretic energy was examined in terms of equivalent viscous damping, which, given a single load-displacement cycle can be expressed as a function of the dissipated energy W_d and the elastic energy at peak displacement W_e : $\xi_{eq} = W_d / 2\pi(W_e^+ + W_e^-)$.

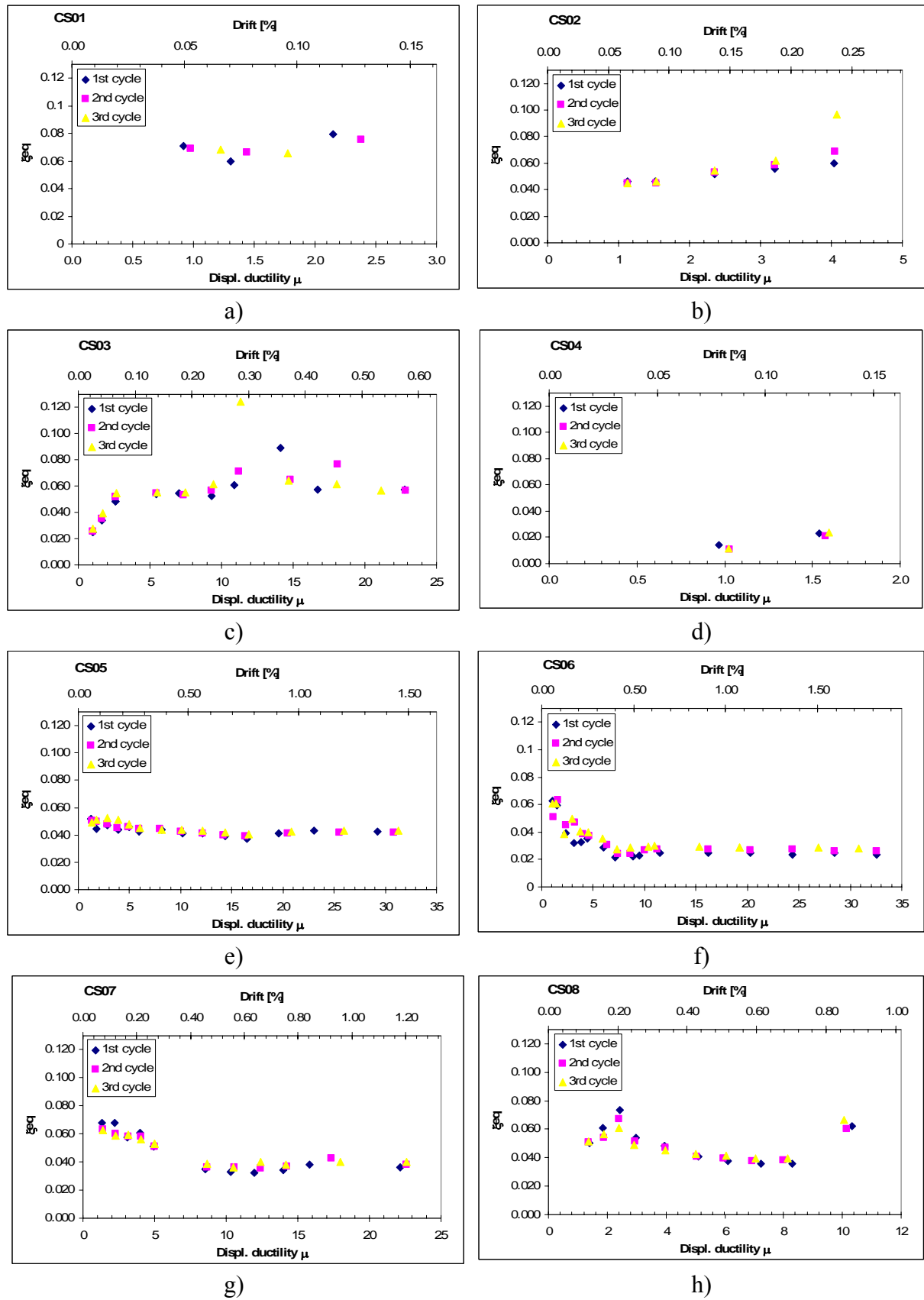


Figure 12. Equivalent viscous damping ratio calculated from the hysteresis loop as a function of ductility ($\mu = \delta / \delta_e$), where δ is the maximum displacement of the cycle.

In Figure 12 the results of the calculated equivalent viscous damping ξ_{eq} are plotted as a function of the displacement ductility (δ/δ_e) and of the drift (δ/H) of each cycle and considering the first, the second and the third cycle at each target displacement.

Except for wall CS07, the equivalent viscous damping ξ_{eq} associated to the cycles corresponding to failure (ultimate) was not plotted.

It may be observed that the cycles have low dissipativity both for shear failures and for flexural failures. The equivalent viscous damping ξ_{eq} was found to be less than 7-8% for almost all cycles, most often around 4%. In wall CS04 very small dissipation occurred, since the wall, before shear failure, behaved essentially in the elastic range. No clear distinction between flexural and shear failure can be noticed looking at the ξ_{eq} - μ plots.

CONCLUSIONS AND FUTURE DEVELOPMENTS

The results of the first part of an experimental campaign on in-plane cyclic behaviour of unreinforced masonry walls have been presented. Tests were carried out on walls made of calcium silicate blocks with thin layer mortar and the results are here discussed in terms of deformation and energy dissipation capacity. The results represent a useful reference for seismic design purposes.

A wide variation in ductility and drift capacity has been reported depending on the failure mode which is in turn influenced by geometry, level of axial load and boundary conditions. When diagonal cracking in units is avoided, high drift capacities can be attained, sometimes exceeding 1.0% or more, whereas very brittle behaviour is reported when diagonal cracks develop through the units. In particular, very low drift capacity (below 0.2%) was reported in presence of high mean vertical compression stress (2 MPa). It appears therefore as an important seismic design criterion to limit compression stresses in walls to avoid bad performance, since the increase in shear strength due to axial compression may not compensate the dramatic reduction in deformation capacity.

Further work will be dedicated to the interpretation of the results in terms of measured strengths, especially important for the walls that displayed diagonal cracking failure and hybrid failure mechanisms. The present experimental campaign will be also integrated by further in-plane tests on walls with different units and materials, for a total of 27 specimens.

ACKNOWLEDGEMENTS

The work has been developed in the ESECMaSE Project funded by the European Commission within the Sixth Framework Programme (Horizontal Research Activities involving SME's – Collective Research Project N°: 500291-2) www.esecmase.org.

REFERENCES

- [1] Kalksandstein – Bundesverband Kalksanstein Industrie eV. : www.kalksandsteind.de
- [2] Magenes, G. and Calvi, G.M., (1997) In-plane seismic response of brick masonry walls, *Earthquake Engineering and Structural Dynamics*, Vol. 26, 1091-1112.
- [3] Tomažević, M. Lutman, M, Petković, (1993) Seismic behaviour of masonry walls: experimental simulation, *J.Struct. Enrg.*, ASCE, 122 (9), 1040-1047.
- [4] Grabowski, S. (2005), D 5.5 Material properties for the tests in WP 7 and 8 and the verification of the design model of WP 4. *Report of WP 5; Project ESECMaSE*.